Geometric and electronic structure of the N/Rh(100) system by core-level photoelectron spectroscopy: Experiment and theory

Laura Bianchettin and Alessandro Baraldi*
Physics Department and Center of Excellence for Nanostructured Materials, Trieste University, Trieste, Italy and Laboratorio TASC INFM-CNR, S.S. 14 Km 163.5, I-34012 Trieste, Italy

Stefano de Gironcoli
SISSA-Scuola Internazionale Superiore di Studi Avanzati and INFM Democritos National Simulation Center, via Beirut 2-4, 34014 Trieste-Grignano, Italy

Silvano Lizzit and Luca Petaccia
Sincrotrone Trieste S.C.p.A., S.S. 14 Km 163.5, 34012 Trieste, Italy

Erik Vesselli, Giovanni Comelli, and Renzo Rosei
Physics Department and Center of Excellence for Nanostructured Materials, Trieste University, Trieste, Italy and Laboratorio TASC INFM-CNR, S.S. 14 Km 163.5, I-34012 Trieste, Italy
(Received 28 March 2006; revised manuscript received 14 June 2006; published 28 July 2006)

The nitrogen interaction with Rh(100) was studied by combining high-energy resolution core level photoelectron spectroscopy and density functional calculations. Nitrogen-induced Rh3$d_{5/2}$ surface core level shifts depend on the N-Rh local geometrical configuration. The core level shifts are dominated by initial state effects and correlate strongly with the variation of the energy position of the surface atom-projected *d*-band center.

DOI: 10.1103/PhysRevB.74.045430 PACS number(s): 68.43.Fg, 73.20.−r, 79.60.−i, 71.15.Mb

I. INTRODUCTION

The interaction of nitrogen with transition metal surfaces has a strong relevance in all catalytic processes involving N-containing species such as N_2, NO, NH_3, and CN. Among the catalysts used in the car exhaust purification (NO+CO reaction), Rh not only exhibits a large activity, but also an extraordinary selectivity towards N_2 production. Atomic nitrogen is also relevant for the formation of cyanide intermediates (which have been detected, as unwanted products, in the catalytic reduction of NO by C_2H_4 on Rh (Refs. 1 and 2)) or in the formation of N_2O, a gas which contributes to the ozone layer depletion and to the greenhouse effect. Moreover, atomic N is an intermediate species in the ammonia oxidation process and in the Ostwald process, in which it is converted to NO by using bimetallic transition metal catalysts. Despite this importance, however, the role of atomic nitrogen in several reaction mechanisms (such as in the HCN and the N_2O formation on different Rh based catalysts), is not yet fully understood.[3] At variance with what is commonly believed, Zaera *et al.* have recently reported, for example, that on Rh(111), N_2O is an intermediate species resulting from the reaction between atomic nitrogen and nitric oxide.[4]

Nitrogen adsorption on (110) and (111) Rh surfaces has been investigated by several experimental techniques.[5] One of the most interesting results is the fact that N adsorption on the open (110) plane is accompanied by a substrate $(n\times 1)$ missing row reconstruction,[6,7] with nitrogen atoms sitting in bridge sites.[8,9] On Rh(111) evidence has been reported on the formation of nitrogen islands and preferential reaction of the perimeter atoms via an N+N recombination.[10–12] Only scant information is available instead, on adsorption site geometries, degree of ordering, and islands formation of nitrogen on Rh(100).[1,2] Theoretical calculations[13] have predicted that nitrogen atoms on Rh(100) (as many other atomic adsorbates do[14]) sit at the highest coordination fourfold hollow site. The chemisorption energy decreases only slightly as the surface coverage increases, and the N adsorption does not induce any substrate reconstruction of the Rh(100) surface,[15] as oxygen does.[16,17] By exposing a Rh(100) surface to a mixture of CO and NO (at temperatures above the nitric oxide desorption but below the onset of N_2 desorption), a N-$c(2\times 2)$ ordered structure forms, with a maximum nitrogen coverage of 0.5 ML, as shown by low energy electron diffraction (LEED) and temperature programmed desorption experiments.[18]

In this study, we present a detailed investigation of the surface geometric and electronic structure of the N/Rh(100) adsorption system, by using high energy resolution core level photoelectron spectroscopy. We show that the analysis of the N1*s* signal and of the nitrogen-induced Rh3$d_{5/2}$ surface core level shifts (SCLSs), provides a clear insight into the process of adlayer formation and on the coverage dependence of the nitrogen adsorption site.

This approach has already been used for a large variety of chemisorption systems on single crystal Rh surfaces, ranging from diatomic molecules such as carbon monoxide,[19–22] to atomic adsorbates like oxygen,[23–25] and hydrogen[26,27] on Rh as well as on other transition metal surfaces.

Our experimental investigation is paralleled by first-principles theoretical calculations of the SCLSs. Our theoretical results (which take into account the initial and final state effects in the electron core level binding energy determination), accurately reproduce both the trends and magnitude of the experimental shifts, and indicate that the N-induced

SCLSs on Rh, mainly originate from initial state effects. These, in turn, are strongly correlated with the Rh 4*d* valence band width change, and with the energy shift of the *d*-band center, upon nitrogen adsorption. The almost linear increase of the SCLSs with increasing the N coordination with Rh atoms suggests that the type of bonding does not change significantly over the whole coverage range up to saturation.

II. EXPERIMENTAL

A. Experimental setup

The core level photoemission measurements have been performed at the SuperESCA beamline of the high-brilliance synchrotron radiation source Elettra. Rh3$d_{5/2}$ and N1*s* core level spectra have been acquired at photon energies of 400 and 470 eV, respectively. A double pass hemispherical electron energy analyzer with 150 mean radius,[28] equipped with a 96 channels detector, has been used to collect the spectra. The overall energy resolution was, respectively, 70 and 200 meV, for the Rh3*d* and the N1*s* spectra. Sample temperature during measurements was maintained at 100 K in order to minimize the vibrational/phonon broadening. In the data we present, binding energies are always referred to the Fermi energy position, measured under the same experimental conditions (photon energies, analyzer setup, and surface temperature). The background pressure in the UHV experimental chamber, during measurements, was always in the low 10^{-10} mbar range. The Rh sample, an 8 mm diameter disk oriented along the (100) direction within 0.1°, has been cleaned by cycles of Ar^+ sputtering ($T=300$ K, $E=3$ keV), annealing at 1320 K, oxygen treatment ($T=570-1070$ K, $p=5\times10^{-8}$ mbar) and a final annealing in hydrogen to remove residual oxygen ($T=470-770$ K, $p=1\times10^{-7}$ mbar). This procedure yields a well ordered and clean surface, as evidenced by sharp and low background (1×1) LEED spots, and by the absence of contaminant traces in the C1*s*, S2*p*, and O1*s* core level regions.

A N adlayer can be prepared on Rh(100) in two different ways: (i) dissociative adsorption of ammonia followed by hydrogen removal by thermal desorption or by oxidation via the reaction

$$3O_2 + 4NH_3 \rightarrow 4N_a + 6O_a + 12H_a \rightarrow 6H_2O_g + 4N_a;$$

(ii) dissociative adsorption of nitric oxide followed by removal of the oxygen by CO

$$NO + CO \rightarrow N_a + O_a + CO_a \rightarrow CO_{2g} + N_a$$

or H_2 reduction

$$NO + H_2 \rightarrow N_a + O_a + 2H_a \rightarrow H_2O_g + N_a.$$

By using the second method, Hardevel *et al.*[2] obtained a long-range ordered $c(2\times2)$ structure, corresponding to a surface coverage of 0.5 ML. We used this last approach. A mixture of NO ($p=5\times10^{-9}$ mbar) and H_2 ($p=1\times10^{-7}$ mbar) was dosed at 550 K, i.e., below the N recombination temperature, which is known to occur above 600 K.[29,30] Once saturated, the surface was annealed to higher temperatures in order to induce nitrogen desorption and obtain progressively lower coverage adlayers.

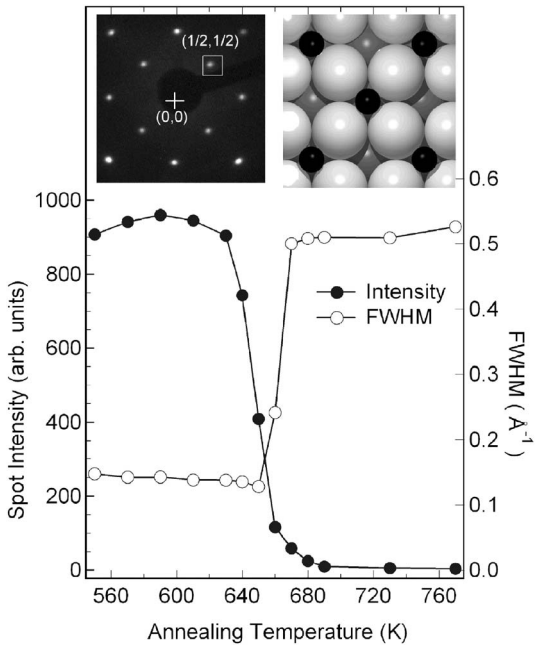

FIG. 1. Intensity (filled circles) and full width at half maximum (empty circles) of the (1/2,1/2) diffraction spot measured at 100 K after annealing at different temperatures. In the top panels an LEED image taken at $E=108$ eV (left) and a model for the $c(2\times2)$ structure (right) are reported.

B. Adlayer characterization

We have performed a first set of LEED and x-ray photoelectron spectroscopy measurements in order to obtain a preliminary characterization of the system. By measuring (at 100 K) the intensity of the (1/2,1/2) LEED spot, characteristic of the $c(2\times2)$ structure, we have monitored the evolution of the adlayer after subsequent annealing at increasing temperatures. The results are shown in Fig. 1.

These results indicate that the 0.5 ML adlayer is thermally stable up to about 630 K, while at higher temperatures a process of desorption/reorganization of the adsorbate takes place. After heating to about 680 K, the $c(2\times2)$ structure disappears and a transition to a (1×1) phase occurs. The diffraction intensity change is accompanied by a parallel increase in the full width at half maximum (FWHM) of the (1/2,1/2) spot, indicative of a disordering process. For annealing temperatures higher than 680 K, the presence of low intensity and very diffuse $(n+1/2,m+1)$ diffraction spots indicates that in the low coverage range, nitrogen on Rh(100) does not form a well ordered $p(2\times2)$ structure as atomic oxygen[31] and sulfur[32] do. For increasing the annealing temperature, we observed just the diffraction spots of the (1×1) substrate, thus indicating that for $\Theta\leqslant0.2$ ML the layer is disordered. Starting from the saturated layer (corresponding to 0.5 ML coverage), after each heating step the N1*s* core level spectra were measured at 100 K, as in the LEED experiment. The spectra reported in Fig. 2(a) show, as ex-

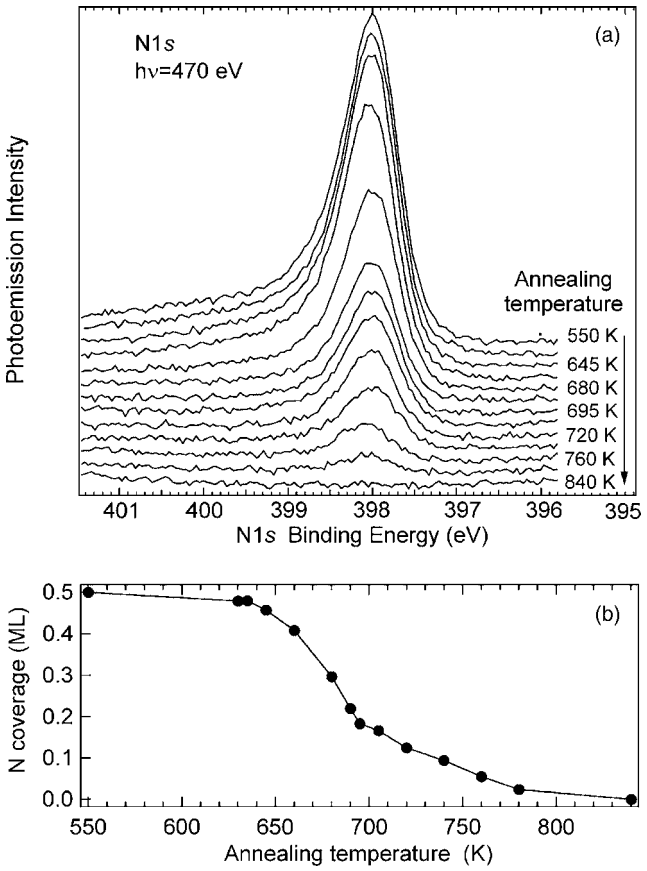

FIG. 2. (a) N1*s* core level spectra measured at $T=100$ K, corresponding to layers with different N coverage, obtained by annealing the initial $c(2\times2)$ structure at progressively higher temperatures. (b) Nitrogen coverage after annealing the surface at even higher temperatures.

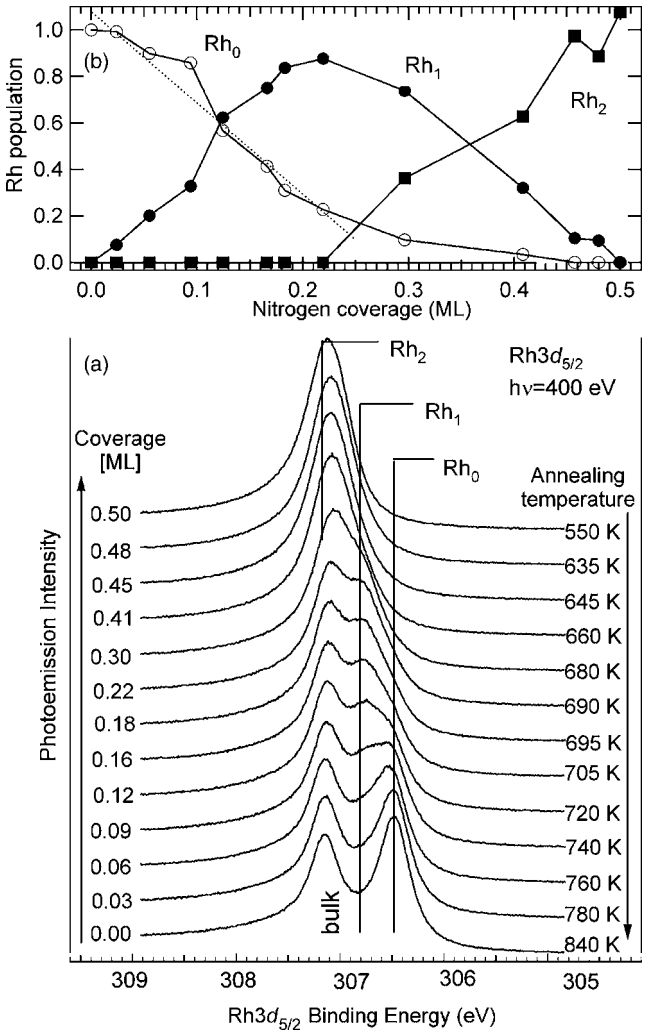

FIG. 3. (a) Rh3$d_{5/2}$ core level spectra measured at $T=100$ K, corresponding to layers with different N coverage, obtained by annealing the initial $c(2\times2)$ structure at progressively higher temperatures. (b) Evolution of the core level intensities corresponding to surface Rh atoms in different local configurations. Note the intercept of the Rh_0 component linear fit (dotted line) at about 1/4 ML.

pected, that the surface coverage diminishes for increasing annealing temperatures and that nitrogen is almost completely desorbed at 840 K, see Fig. 2(b).

The photoemission data have been fitted by a convolution of a Doniach Sunjic (DS) function[33] and a Gaussian, which account for the vibration/phonon and many-body effects, and the contribution of the instrumental resolution, respectively. A linear background was also subtracted. The DS profile contains a Lorentzian distribution (described by the Γ parameter) arising from the finite core-hole lifetime, and an asymmetry parameter α for electron-hole pairs excitation at the Fermi level. In the entire coverage range the N1*s* spectra show just a single peak, always at a binding energy (BE) of 398.1 eV, within the experimental error bar of ±50 meV. This peak can be associated to a N species which occupies the same adsorption site in the whole coverage range. The N1*s* BE we measured is about 0.8 eV larger than the N1*s* BE found for a N+O coadsorbed layer on the same surface[34] and this probably reflects the influence of interatomic interactions between the adspecies and/or different N local environment. The occupation of the same adsorption site, independent from the nitrogen coverage, is in agreement with the results of Loffreda *et al.*,[13] which show that the highest coordination fourfold hollow site is always the most stable geometry. The comparison between LEED and core-level experiments proves that the $c(2\times2)$ structure requires a critical coverage of about 0.4 ML to develop.

C. The Rh3$d_{5/2}$ core level spectra

Atomic adsorbate core levels are not very sensitive to small modifications of the atom-metal bond. Therefore, in order to understand the evolution of the local nitrogen atoms configuration, along with the variations of the electronic structure of substrate Rh atoms, we have made extensive measurements of the Rh3$d_{5/2}$ core level spectra.

Figure 3(a) shows a sequence of spectra corresponding to different nitrogen coverage, from the clean surface (bottom), to the $c(2\times2)$ structure (top). The annealing temperature and nitrogen coverage are reported for each curve. As already reported,[27,35–39] the spectrum corresponding to the clean (1×1) Rh(100) surface is composed by two peaks: the higher

BE component at 307.15 eV, originates from subsurface and deeper layers, while the lower BE peak (Rh_0), at -660 ± 20 meV with respect to the bulk peak, originates from topmost Rh atoms. A two component analysis gives, respectively, best fit values for the Γ, α and Gaussian width parameters, of 0.26, 0.16, and 0.13 eV for the bulk, and 0.28, 0.23, and 0.13 eV for the surface component.[40]

In order to evaluate the position and intensity of the different nitrogen-induced surface core level shifted components we performed a fit of the Rh3$d_{5/2}$ spectra for the nitrogen covered surfaces in the same way as for the clean surface case. We find that all the spectra can be properly fit by adding only two new surface components, as revealed by the low fitting residual and by the chi-square analysis. Low nitrogen coverage ($\leqslant$0.2 ML) leads to the appearance of a second surface core level component, Rh_1, shifted by -360 ± 20 meV with respect to the bulk one, while the original surface peak intensity decreases. Upon increasing the nitrogen coverage we observe a further decrease of Rh_0, accompanied by the growth of a third surface component, Rh_2, at a binding energy very close to the BE of the bulk component. For this reason, its position can be determined with lower accuracy ($+10\pm30$ meV).

In order to determine the initial nitrogen adsorption site we apply the method we recently developed,[24] which is based on the analysis of the coverage dependent behavior of the Rh_0 clean surface component integrated intensity. The results of the data analysis are reported in Fig. 3(b). If we neglect photoelectron diffraction effects, the intensity variations of the different components with N coverage reported in Fig. 3(b) reflect the variation in the population of differently coordinated Rh atoms. At low N coverage the number of Rh_1 atoms linearly increases with nitrogen coverage at the expense of the Rh_0 population. The Rh_2 component starts growing later, at coverage larger than 0.2 ML. Only at saturation do the Rh_0 and Rh_1 components disappear, when the Rh_2 population reaches its maximum. In particular we note that the first derivative $\frac{dRh_0}{d\Theta}$ is equal to -3.9 ± 0.4, which indicates that for each N atom adsorbed on the surface, the intensity contribution of approximately four surface Rh atoms moves from Rh_0 to Rh_1. Therefore the adsorption site can be directly assigned to the fourfold hollow, as predicted by theory.[13,15] The N-induced surface core level shifted components are interpreted as originated by first layer Rh atoms, one directly bonded to a single nitrogen adatom (Rh_1) and the other double-bonded with nitrogen (Rh_2). At saturation all the Rh atoms in the $c(2\times2)$ arrangement result to be double-bonded with N atoms in the geometrical configuration depicted in Fig. 1 (top). The onset of Rh_2 population only at a finite coverage [$>$0.2 ML in Fig. 3(b)] indicates, in agreement with theoretical findings (Ref. 13) that the nearest-neighbor and next-nearest neighbor interactions are repulsive on this surface. This model is simplified as it only considers the coordination of the Rh atoms, while possible differences in the local geometrical environment due to nitrogen induced lateral and vertical displacements of the Rh atoms in the outermost layers are ignored.

III. THEORY

A. Methods

In order to obtain a deeper understanding of the origin of the nitrogen-induced surface core level shifted components and to verify the SCLS experimental assignment we studied theoretically the N adsorption on Rh(100). The calculations have been performed using density functional theory (DFT)[41] based on the local density approximation (LDA) of the exchange-correlation functional in the Ceperley and Alder form[42] as parametrized by Perdew and Zunger.[43] The Kohn-Sham equations are solved self-consistently using a plane-wave basis set restricted to a kinetic energy cutoff of 30 Ry, in an ultrasoft (US) pseudopotential scheme,[44] as implemented in the Quantum-ESPRESSO open-source distribution.[45] The Rh(100) surface has been modeled by a seven-layer slab with a vacuum region corresponding to five interlayer spacings. Nitrogen atoms are adsorbed on one side of the slab, allowing full relaxation except for the in-plane lattice parameter that is kept fixed to its calculated bulk equilibrium value. To deal with the metallic character of the system, we have used a Methfessel and Paxton smearing function[46] of order 1 with a width $\sigma=0.03$ Ry and a $(12\times12\times2)$ Monkhorst-Pack grid for the (1×1) surface unit cell, resulting in 21 special k points in the irreducible wedge.[47] Equivalent k point samplings have been used when dealing with larger supercells.

B. Geometric and electronic structure

The nitrogen interaction with Rh(100) was modeled by using three different supercells, a $(2\sqrt{2}\times2\sqrt{2})$, a $p(2\times2)$, and a $c(2\times2)$, which correspond to coverage of $\theta=0.125$, 0.25, and 0.5 ML, respectively. The $(2\sqrt{2}\times2\sqrt{2})$ and $p(2\times2)$ structures were used, just for computational convenience, to describe the low coverage behavior. Indeed LEED results have shown that at 0.25 ML nitrogen does not form a long-range well ordered $p(2\times2)$ layer and at lower coverage the system is disordered. This choice does not affect the overall results since we are interested in the local electronic properties as measured by surface core level shift, which are known to be strongly dependent on the local environment. The nitrogen atoms have been positioned always in the fourfold hollow sites, in agreement with present experimental evidence and previous theoretical work.[13,15] The structures, shown in Fig. 4, involve first layer Rh atoms which are "clean" or bonded with one or two N atoms. As it will be explicitly shown in the following these different Rh moieties are indeed responsible, as suggested by the experimental analysis, for the Rh_0, Rh_1, and Rh_2 components in the Rh3$d_{5/2}$ spectra of Fig. 3. It is important to notice that second layer Rh atoms are in a different local environment, as shown by different labeling in Fig. 4, and therefore are expected to produce different subsurface core level shifted components.

The calculated nitrogen equilibrium geometries in the three different structures are reported in Table I. The nitrogen adsorption height is very similar in the three different phases, varying from 0.65 Å at 0.125 ML to 0.68 Å at 0.5 ML, re-

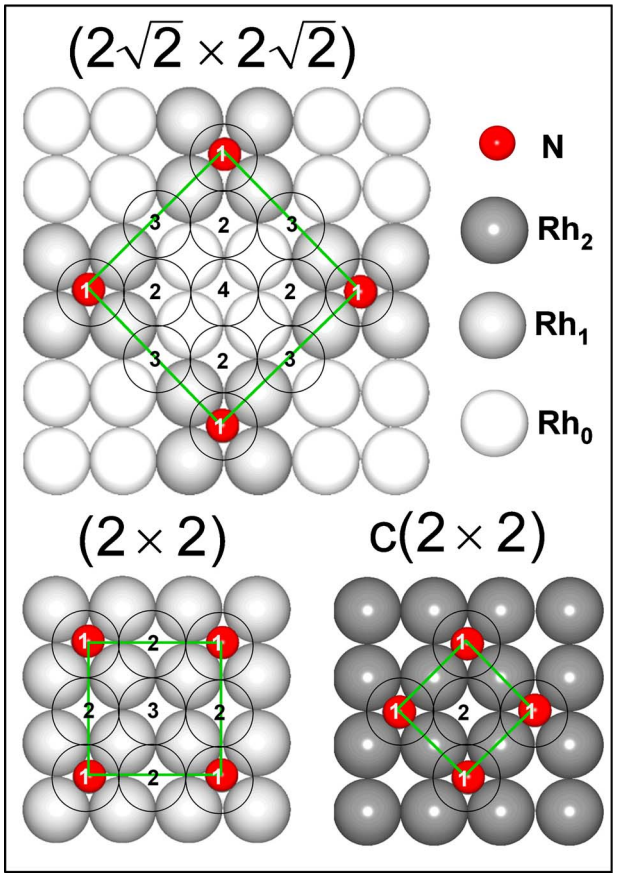

FIG. 4. (Color online) Structural configurations for N adsorbed in the fourfold hollow site: first layer Rh atoms (Rh_0 clean, Rh_1 bonded to 1 N atom, and Rh_2 bonded to 2 N atoms), are reported with different colors. Inequivalent atoms in the second layer are labeled 1–4. (a) $(2\sqrt{2}\times 2\sqrt{2})$ (θ=0.125 ML); (b) (2×2) (θ=0.25 ML) and (c) $c(2\times 2)$ (θ=0.5 ML).

sulting in a 2.00 Å N-Rh bond length. For comparison with other Rh surfaces, this distance results to be, respectively, 7% and 9% larger than the N-Rh interatomic distance when N is adsorbed in bridge sites on Rh(110) (1.87 Å)[8,9] or in threefold hollow sites on Rh(111) (1.84 Å).[48] At saturation coverage the reported structure is in good agreement with previous theoretical determinations.[13,15]

The nitrogen chemisorption on Rh(100) is originated by the formation of a covalent bond between N and the substrate atoms. Because of the narrow *d* band of transition metals, the interaction of atomic nitrogen with the *d* electrons gives rise to bonding and antibonding states, with the N-TM bond strength increasing when the *d*-band width decreases.[49] In Fig. 5 we report the projected density of states (PDOS)[50] on the p_x and p_z nitrogen-atom orbitals and Rh $d_{x^2-y^2}$, d_{xz}, and d_{xy} orbitals for the Rh+N system corresponding to the structures at 0.125 and 0.5 ML (for symmetry reasons the p_x and p_y orbitals are equivalent). It is possible to observe the presence of resonances with the p_x and p_z orbitals above (2 eV) and below (−7 eV) the Fermi level, with empty antibonding states indicating a strong N chemisorption.

Nitrogen-surface bonding is also partly ionic with some charge transfer from the surface to the adsorbate, originating

TABLE I. Calculated structural parameters (in Å) for the three different structures with N atom sitting in fourfold hollow sites. Vertical distance between the adsorbate and the plane of the four Rh atoms defining the fourfold site is denoted as d_{Rh_i-N} (i=0,1,2). The first-to-second layer distance is Δd_j, where j varies from 1 to 4 and represents all the inequivalent atoms in the second layer (see Fig. 4). The distance between first and second layer for the clean Rh(100) surface is 1.82 Å, while d_{bulk}=1.89 Å. Values in parentheses correspond to relaxations with respect to the bulk distance.

	0.125 ML	0.25 ML	0.5 ML
d_{Rh_0-N}	0.73		
d_{Rh_1-N}	0.65	0.68	
d_{Rh_2-N}			0.68
Δd_1	1.91 (+1%)	1.95 (+3.2%)	1.99 (+5.2%)
Δd_2	1.86 (−1.6%)	1.90 (+0.5%)	1.99 (+5.2%)
Δd_3	1.85 (−2.1%)	1.86 (−1.6%)	
Δd_4	1.85 (−2.1%)		

from the large difference in electronegativity[51] $\Delta\mu$=0.76 between Rh (μ=2.28) and N (μ=3.04) atoms. For the 0.5 ML structure we found a charge donation equal to 0.5 e^- towards the nitrogen atom.[52]

Nitrogen adsorption induces a considerable surface relaxation. The height of the inequivalent second-layer atoms, la-

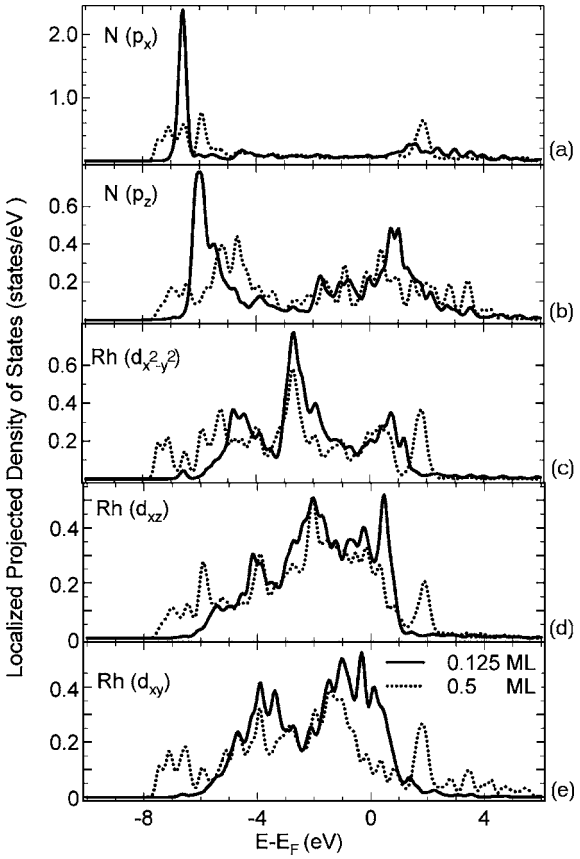

FIG. 5. Projected local density of states on the (a) p_x and (b) p_z N orbitals, and on the (c) $d_{x^2-y^2}$, (d) d_{xz}, and (e) d_{xy} orbitals of the surface Rh atoms (Rh_0 at 0.125 ML and Rh_2 at 0.5 ML).

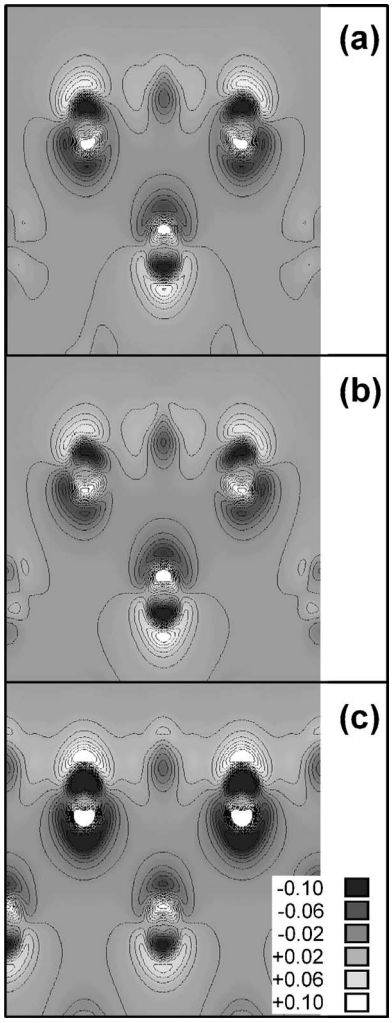

FIG. 6. Contours of constant charge density (see Ref. 63), in a (010) plane perpendicular to the (100) surface of N/Rh and along the bonding direction. Contours correspond to a charge-density difference $\Delta n = n[(\mathrm{Rh+N}) - n(\mathrm{Rh}) - n(\mathrm{N})]$. The difference between constant-density contours is 0.013 $e/(ua)^3$. (a) $\Theta = 0.125$ ML $(2\sqrt{2} \times 2\sqrt{2})$ structure; (b) $\Theta = 0.25$ ML (2×2) structure (c) $\Theta = 0.5$ ML $c(2\times2)$ structure.

beled 1, 2, 3, and 4 in Fig. 4, varies by up to 0.07 Å for the $(2\sqrt{2}\times2\sqrt{2})$ structure and up to 0.08 Å for the (2×2). The second layer-atoms in the $c(2\times2)$ structure are coplanar, with the first-to-second layer distance increased by a large amount (0.1 Å, i.e., +5%).

These findings are a manifestation of the general tendency of electronegative species to weaken the Rh-Rh bonds thus producing an expansion of the first interlayer distance upon adsorption. This can be observed directly in Fig. 6, which shows contour plots of constant charge density, in the (010) plane perpendicular to the (100) surface, of the charge-density difference between the chemisorbed systems ((a) 0.125 ML, (b) 0.25 ML, and (c) 0.5 ML) and the sum of the charge densities of the clean Rh(100) surface and the isolated N atom. The reduced electron density between the two outermost substrate layers upon N adsorption, which empties the Rh-Rh bonding states is at the origin of the mentioned large expansion of the first-to-second layer distance d_{12} with respect to the relaxed clean surface.

C. Surface core level shift calculations

The SCLS is defined, including final-state effect, as the difference between the binding energy (BE) of a core electron in a bulk atom, BE_{bulk}, and the one in a surface atom BE_{surf}:

$$\mathrm{SCLS} = \mathrm{BE}_{bulk} - \mathrm{BE}_{surf},$$

where the BE is the all-electron total energy E^{AE} difference between the final state (i.e., the system with $(\mathrm{N}-1)$ atoms in the ground state and one excited atom) and the initial state (i.e., the system with N atoms in the ground state):

$$\mathrm{BE} = E^{AE}((\mathrm{N}-1)\mathrm{Rh}, 1\mathrm{Rh}^{\star}) - E^{AE}(\mathrm{NRh}, 0\mathrm{Rh}^{\star}).$$

Final state core level BE can be accurately computed also in the pseudopotential formalism adopted here by describing the excited atom by a pseudopotential generated in the core-excited configuration.[53] In this formulation the core-level BE is given by the pseudopotential total energy difference supplemented by an additive constant that can be determined for the isolated atom

$$\mathrm{BE} = E^{PS}((\mathrm{N}-1)\mathrm{Rh}, 1\mathrm{Rh}^{\star}) - E^{PS}(\mathrm{NRh}, 0\mathrm{Rh}^{\star}) + [E^{AE}_{at}(\mathrm{Rh}^{\star}) - E^{PS}_{at}(\mathrm{Rh}^{\star}) - E^{AE}_{at}(\mathrm{Rh}) + E^{PS}_{at}(\mathrm{Rh})]$$

and cancels out when comparing different geometries:

$$\mathrm{SCLS} = E^{PS}_{bulk}((\mathrm{N}-1)\mathrm{Rh}, 1\mathrm{Rh}^{\star}_{bulk}) - E^{PS}_{surf}((\mathrm{N}-1)\mathrm{Rh}, 1\mathrm{Rh}^{\star}_{surf}).$$

The latter is the quantity to be compared with the experimental shifts.

Isolated $\mathrm{Rh}^{\star}$ excited atoms are simulated by supercells so as to minimize the interaction of the excited atom with its periodic replicas. For one test configuration ($\theta = 0.25$ ML) SCLS were computed on a set of supercells of sequentially increasing size, i.e., a (2×2), a $(2\sqrt{2}\times2\sqrt{2})$ and a (4×4) in-plane periodicity. We obtained a SCLS value of −306, −286, and −282 meV, respectively, and concluded that a $(2\sqrt{2}\times2\sqrt{2})$ periodicity is sufficient to have a very good numerical accuracy (a few meV), while the smaller cell is inadequate to describe the system to such an accuracy. Another possible source of numerical error is the finite thickness of the vacuum region between the repeated slabs. We relaxed the $\theta = 0.25$ ML system for two slabs with a vacuum region corresponding to 5 and 6 Rh layers and we found that the total energy and the atomic positions were unchanged within 1 mRy and 6×10^{-3} Å, respectively. The smaller slab was therefore used.

IV. DISCUSSION

Our calculated SCLS for the clean Rh(100) surface is −580 meV. The analysis of the experimental data (based on a fitting procedure using only two components), gives a value of −660 meV. This agreement between theory and experiment is already quite satisfactory, but it can be significantly improved if we consider explicitly the spectral contribution

TABLE II. The Rh $3d_{5/2}$ surface-core level shifts (meV) at the (100) surface of Rh, as obtained by the full and the initial state calculations, for the differently N-coordinated first layer Rh atoms, and for the inequivalent second layer atoms (see Fig. 4). For the second layer atoms at the lowest coverage, only initial state contributions were computed. The calculated shifts of the *d*-band center (with respect to bulk *d* band), are also given.

Coverage	Rh atom	Full cal.	Initial state	ΔB_d
Clean	Rh_0	−580	−650	−578
	II layer	+140	+80	+101
0.125	Rh_0	−577	−604	−570
	Rh_1	−329	−396	−391
	II-layer (1)		−16	+34
	II-layer (2)		+159	+144
	II-layer (3)		+73	+59
	II-layer (4)		+48	+43
0.25	Rh_1	−286	−346	−369
	II-layer (1)	+47	+51	+89
	II-layer (2)	+55	+66	+39
	II-layer (3)	+22	−19	−17
0.5	Rh_2	+62	−3	−70
	II-layer (1)	−103	−93	−30
	II-layer (2)	−99	−29	−47

of the second layer of Rh atoms. Our DFT calculations give a second layer Rh atoms SCLS (with respect to the bulk peak), of +140 meV. This suggests that our simple two-peak fitting procedure overestimates systematically the first layer SCLS. Indeed, we have repeated the analysis with a three component fit of the Rh(100) clean surface spectrum, and we find a first layer SCLS component at −600 meV and a second layer component at +100 meV, thus bringing theory and experiment in much better agreement. A similar situation has been previously found for the Rh(111) surface, where the second layer spectral contribution was determined at (+71 meV),[54] and theoretically calculated at (+67).[23]

We carried out initial[55] and full calculations of the 3*d* SCLSs for each inequivalent Rh atom in the two outermost layers for the clean Rh(100) surface, and for the structures at 0.125, 0.25, and 0.5 ML nitrogen coverage. Initial-state SCLS of any atom in a system can be easily calculated from the ground state self-consistent overall electronic structure solution. Final-state contributions require, instead, a separate calculation for each atom of interest, and is therefore a much more demanding task. For this reason, only initial-state SCLS were computed for the spectral components of some of the second layer Rh atoms at the lowest nitrogen coverage. The results are reported in Table II.

The contribution of electronic screening effects (obtained as the difference between the full and the initial-state values), are always relatively small ($\leqslant$70 meV), showing that the initial-state effects are predominant.

This fact, previously reported also for the oxygen induced Rh $3d_{5/2}$ SCLSs on Rh(111), simplifies the interpretation of the shifts physical origin. The negative SCLS of the clean (100) surface, for instance, can be easily explained by the reduced *d*-band width, originating from the lower coordination number of the surface, with respect to bulk atoms. Assuming an approximate conservation of the *d* charge in each layer, the *d* band at the surface has to be shifted relative to the bulk band.[60] For Rh, which has a more than half filled *d* band, the shift is upward, resulting in a negative SCLS.

The results in Table II clearly indicate that, for the nitrogen structures on Rh(100), there is a strong dependence of SCLSs on the Rh atom-adsorbate coordination, as previously shown for oxygen on different transition metals.[23,24,56] Our calculations show also that subsurface atoms contribute with shift values ranging from −103 up to +159 meV.[57] This makes it difficult to include them properly in a fitting procedure of the experimental spectra.

A fair comparison between experimental and theoretical results can be done by considering the shifts ΔE_i of the N-induced surface core-level shifted components Rh_i with respect to the clean Rh_0 component, whose BE can be experimentally determined with high accuracy. The experimental values $\Delta E_1 = 300 \pm 40$ meV and $\Delta E_2 = 670 \pm 60$ meV result to be in very good agreement with the theoretical ones, $\Delta E_1 = 251 - 296$ meV (254–304 meV) and $\Delta E_2 = 642$ meV (647 meV) for final (initial) state calculations listed in Table II, demonstrating the usefulness and reliability of our combined experimental-theoretical approach. The present results indicate that, also for N-Rh(100), $\Delta E_2 \approx 2\Delta E_1$, thus confirming a model previously put forward for other adsorbates systems.[24,26,27]

The shift toward higher binding energies as N coverage increases is expected for the chemisorption of electronegative species on transition metal surfaces as a consequence of charge transfer from the surface to the adsorbate, however, the increase of the core level shift upon increasing the number of Rh-N bonds cannot be quantitatively accounted for simply by charge transfer. Other effects are known to play a

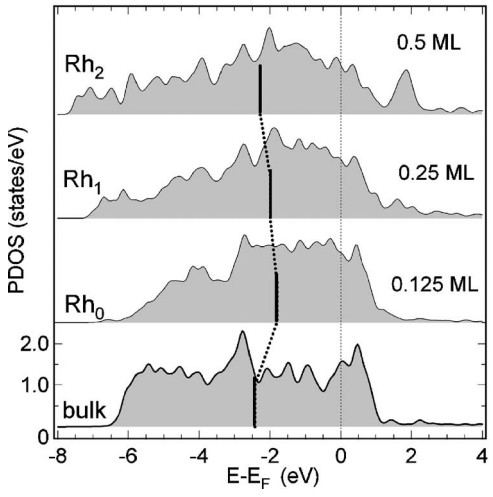

FIG. 7. Projected density of states per Rh atom onto the 4*d* orbitals for all the inequivalent surface atoms at 0.125 and 0.50 ML coverage. Rh_0 atoms are not bound to nitrogen; Rh_1 and Rh_2 are Rh atoms single- and double-coordinated with N. Bottom panel shows the projection corresponding to Rh bulk atoms. Thick vertical lines indicate the center of the *d* band.

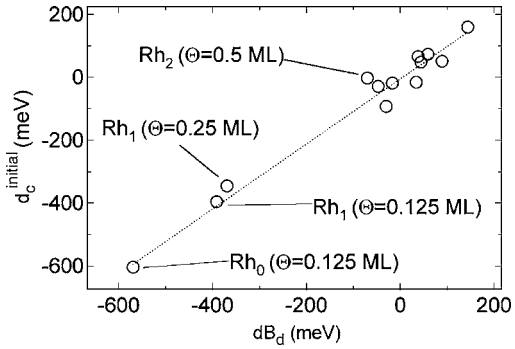

FIG. 8. Calculated initial-state core-level shifts versus shift of the *d*-band center with respect to the bulk *d*-band center. Shifts originated by first-layer atoms are indicated, while the remaining scattered points are originated by inequivalent second-layer atoms. The dotted line serves as a guide to the eyes.

role such as environmental and configurational effects,[56,58,59] stemming from the variation in the local valence electron density and the *sp*-*d* rehybridization upon adsorption. These effects modify significantly the charge transfer contribution but do not revert the trend.

The changes in the surface potential for increasing nitrogen coverage are reflected in the variations in the *d* band of first-layer atoms with respect to bulk ones. In Fig. 7 we plot the calculated density of states (DOS) per atom, projected onto the 4*d* orbitals, for surface (Rh_0) and bulk atoms, as well as for first layer Rh atoms bound to one or two nitrogen atoms. The DOS for the clean surface (Rh_0 type atoms), is narrower than the bulk DOS, and its center is shifted towards the Fermi level. Upon nitrogen adsorption, the *d* DOS of Rh atoms in the Rh_1 configuration, broadens again and its center shifts away from the Fermi level toward higher binding energies. For Rh atoms in the Rh_2 configuration, the *d* DOS broadens even more and its center (reported as a thick vertical line) shifts further to higher binding energies.

Figure 8 shows that the variations of the initial-state SCLSs follow a linear trend with ΔB_d (dotted lines), both quantities originating from the variation of the Kohn-Sham potential.

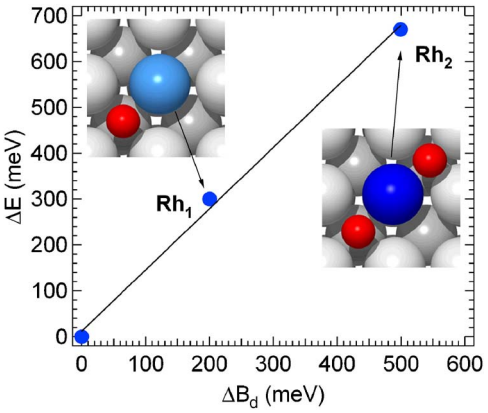

FIG. 9. (Color online) Changes in nitrogen-induced core-level shifts ΔE_i for Rh atoms in the Rh_i configurations (experimental values), versus the calculated atom-projected shift of the *d*-band center.

In Fig. 9 we report on the experimental core level shift for Rh atoms in different configurations (with respect to Rh_0), versus the atom-projected shift of the *d*-band center. As previously found for other adsorbate systems, there is a clear linear relationship among them. Therefore, as long as the core-hole screening contribution in the SCLS and the variations in the local adsorption geometries (interatomic distances, surface relaxations, etc.) are not too large, SCLSs represent a measure of local surface chemical reactivity changes.[61–63]

In conclusion we have shown that a close comparison between high-energy resolution core level photoelectron spectroscopy measurements and density functional theory calculations can be used to understand the nitrogen coverage dependence of both geometric and electronic structure of Rh(100).

We acknowledge financial support from the MIUR under the program PRIN2003 and FIRB. Calculations were performed at SISSA and at the CINECA computing center, also thanks to INFM computing grants.

*Author to whom correspondence should be addressed. Electronic address: alessandro.baraldi@elettra.trieste.it

[1] R. M. Hardeveld, A. J. G. W. Schmidt, R. A. van Santen, and J. W. Niemantsverdriet, J. Vac. Sci. Technol. A **15**, 1642 (1997).
[2] R. M. Hardeveld, R. A. van Santen, and J. W. Niemantsverdriet, J. Phys. Chem. B **101**, 7901 (1997).
[3] V. P. Zhdanov and B. Kasemo, Surf. Sci. Rep. **29**, 31 (1997).
[4] F. Zaera and C. S. Gopinath, Chem. Phys. Lett. **332**, 209 (2000).
[5] G. Comelli, V. R. Dhanak, M. Kiskinova, K. C. Prince, and R. Rosei, Surf. Sci. Rep. **32**, 167 (1998).
[6] G. Comelli, S. Lizzit, P. Hofmann, G. Paolucci, M. Kiskinova, and R. Rosei, Surf. Sci. **277**, 31 (1992).
[7] S. Lizzit, G. Comelli, P. Hofmann, G. Paolucci, M. Kiskinova, and R. Rosei, Surf. Sci. **276**, 144 (1992).
[8] V. R. Dhanak, A. Baraldi, G. Comelli, K. C. Prince, R. Rosei, A. Atrei, and E. Zanazzi, Phys. Rev. B **51**, 1965 (1995).
[9] M. Gierer, F. Mertens, H. Over, G. Ertl, and R. Imbihl, Surf. Sci. **339**, L903 (1995).
[10] F. Zaera and C. S. Gopinath, J. Chem. Phys. **111**, 8088 (1999).
[11] F. Zaera, S. Wehner, C. S. Gopinath, J. L. Sales, V. Gargiulo, and G. Zgrablich, J. Phys. Chem. B **105**, 7771 (2001).
[12] F. Zaera and C. S. Gopinath, J. Chem. Phys. **116**, 1128 (2002).
[13] D. Loffreda, D. Simon, and P. Sautet, J. Chem. Phys. **108**, 6447 (1998).
[14] R. A. van Santen and J. W. Niemantsverdriet, *Chemical Kinetics and Catalysis* (Plenum Press, New York, 1995).
[15] D. Alfé, S. de Gironcoli, and S. Baroni, Surf. Sci. **437**, 18 (1999).
[16] D. Alfé, S. de Gironcoli, and S. Baroni, Surf. Sci. **410**, 151

(1998).
[17] A. Baraldi, J. Cerda, J. A. Martin-Gago, G. Comelli, S. Lizzit, G. Paolucci, and R. Rosei, Phys. Rev. Lett. **82**, 4874 (1999).
[18] A. P. van Bavel, M. J. P. Hopstaken, D. Curulla, J. W. Niemantsverdriet, J. J. Lukkien, and P. A. Hilbers, J. Chem. Phys. **119**, 524 (2003).
[19] A. Beutler, E. Lundgren, R. Nyholm, J. N. Andersen, B. J. Setlik, and D. Heskett, Surf. Sci. **396**, 117 (1998).
[20] M. Birgersson, C. O. Almbladh, M. Borg, and J. N. Andersen, Phys. Rev. B **67**, 045402 (2003).
[21] F. Strisland, A. Beutler, A. J. Jaworowski, R. Nyholm, B. Setlik, D. Heskett, and J. N. Andersen, Surf. Sci. **410**, 330 (1998).
[22] J. N. Andersen and C. O. Almbladh, J. Phys.: Condens. Matter **13**, 11267 (2001).
[23] M. V. Ganduglia-Pirovano, M. Scheffler, A. Baraldi, S. Lizzit, G. Comelli, G. Paolucci, and R. Rosei, Phys. Rev. B **63**, 205415 (2001).
[24] A. Baraldi, S. Lizzit, G. Comelli, M. Kiskinova, R. Rosei, K. Honkala, and J. K. Nørskov, Phys. Rev. Lett. **93**, 046101 (2004).
[25] L. Köhler, G. Kresse, M. Schmid, E. Lundgren, J. Gustafson, A. Mikkelsen, M. Borg, J. Yahara, J. N. Andersen, M. Marsman, and P. Varga, Phys. Rev. Lett. **93**, 266103 (2004).
[26] C. J. Weststrate, A. Baraldi, L. Rumiz, S. Lizzit, G. Comelli, and R. Rosei, Surf. Sci. **566-568**, 486 (2004).
[27] E. Vesselli, A. Baraldi, F. Bondino, G. Comelli, M. Peressi, and R. Rosei, Phys. Rev. B **70**, 115404 (2004).
[28] A. Baraldi and V. R. Dhanak, J. Electron Spectrosc. Relat. Phenom. **67**, 211 (1994).
[29] M. J. P. Hopstaken and J. W. Niemantsverdriet, J. Phys. Chem. B **104**, 3058 (2000).
[30] A. Siokou and J. W. Niemantsverdriet, J. Chem. Phys. **402**, 110 (1998).
[31] A. Baraldi, V. R. Dhanak, G. Comelli, K. C. Prince, and R. Rosei, Phys. Rev. B **56**, 10511 (1997).
[32] L. Bianchettin, A. Baraldi, S. de Gironcoli, E. Vesselli, S. Lizzit, L. Petaccia, G. Comelli, and R. Rosei (unpublished).
[33] S. Doniach and M. Sunjic, J. Phys. C **3**, 185 (1970).
[34] F. Bondino, G. Comelli, A. Baraldi, E. Vesselli, R. Rosei, A. Goldoni, and S. Lizzit, J. Chem. Phys. **119**, 12534 (2003).
[35] F. Strisland, A. Ramstad, T. Ramsvik, and A. Borg, Surf. Sci. **415**, L1020 (1998).
[36] M. Zacchigna, C. Astaldi, K. C. Prince, M. Sastry, C. Comicioli, M. Evans, R. Rosei *et al.*, Phys. Rev. B **54**, 7713 (1996).
[37] J. N. Andersen, D. Hennig, E. Lundgren, M. Methfessel, R. Nyholm, and M. Scheffler, Phys. Rev. B **50**, 17525 (1994).
[38] A. Baraldi, G. Comelli, S. Lizzit, R. Rosei, and G. Paolucci, Phys. Rev. B **61**, 12713 (2000).
[39] A. Goldoni, A. Baraldi, G. Comelli, S. Lizzit, and G. Paolucci, Phys. Rev. Lett. **82**, 3156 (1999).
[40] Line shape parameters are allowed to vary in the fitting procedure of about 10% around the best value obtained in the fit of the clean surface.
[41] P. Hohenberg and W. Kohn, Phys. Rev. **136**, B864 (1964); W. Kohn and L. Sham, Phys. Rev. **140**, A1133 (1965).
[42] D. M. Ceperley and B. J. Alder, Phys. Rev. Lett. **45**, 566 (1980).
[43] J. P. Perdew and A. Zunger, Phys. Rev. B **23**, 5048 (1981).
[44] D. Vanderbilt, Phys. Rev. B **41**, 7892 (1990).
[45] S. Baroni, S. de Gironcoli, A. Dal Corso, and P. Giannozzi, http://www.quantum-espresso.org.
[46] M. Methfessel and A. T. Paxton, Phys. Rev. B **40**, 3616 (1989).
[47] H. J. Monkhorst and J. D. Pack, Phys. Rev. B **13**, 5188 (1976).
[48] M. Mavrikakis, J. Rempel, J. Greeley, L. B. Hansen, and J. K. Nørskov, J. Chem. Phys. **117**, 6737 (2002).
[49] B. Hammer and J. K. Nørskov, Adv. Catal. **45**, 71 (2000).
[50] The PDOS is defined as the projection of the density of states onto the atomic wave function ϕ_i^{at}:

$$n_i(E) = \sum_n \int_{BZ} \delta(E - E_n(\mathbf{k}))|\langle \phi_\mathbf{i}^\mathbf{at}|\psi_\mathbf{n}(\mathbf{k})\rangle|^2 \mathbf{dk},$$

where $\psi_n(\mathbf{k})$ is the crystal wave function of the nth band at wave vector $\mathbf{k}$. In practice the δ function is replaced with a Gaussian of 0.15 eV width.
[51] L. Pauling, *The Nature of the Chemical Bond*, 3rd ed. (Cornell University Press, Ithaca, 1960).
[52] We calculated this value by integrating the PDOS up to the Fermi level.
[53] E. Pehlke and M. Scheffler, Phys. Rev. Lett. **71**, 2338 (1993).
[54] A. Baraldi, S. Lizzit, A. Novello, G. Comelli, and R. Rosei, Phys. Rev. B **67**, 205404 (2003).
[55] In an all-electron framework initial state SCLS is simply the variation of the core eigenvalue before the excitation of the core hole:

$$\Delta_c^{init} \approx \varepsilon_c^{bulk}(n_c) - \varepsilon_c^{surf}(n_c),$$

where $\varepsilon_c^{surf(bulk)}$ is the Kohn-Sham eigenvalue of the core state c in the surface (bulk) atom and n_c is the electron number. In a pseudopotential approach this quantity can be estimated from the linear variation of the total energy when transforming a Rh atom into a Rh^* one.
[56] S. Lizzit, A. Baraldi, A. Groso, K. Reuter, M. V. Ganduglia-Pirovano, C. Stampfl, M. Scheffler, M. Stichler, C. Keller, W. Wurth, and D. Menzel, Phys. Rev. B **63**, 205419 (2001).
[57] +159 meV is the initial state result, but we can safely assume that the full value should be very close, since the calculated screening contributions for the other configurations are always less than 70 meV.
[58] G. A. Benesh and D. A. King, Chem. Phys. Lett. **191**, 315 (1992);
[59] P. S. Bagus, F. Illas, G. Pacchioni, and F. Parmigiani, J. Electron Spectrosc. Relat. Phenom. **100**, 215 (1999).
[60] The d-band center displacement of surface atom with respect to the bulk ones is: $\Delta B_d = B_d^{bulk} - B_d^{surf}$. We define the pth moment of the DOS $n_i(E)$ as $\mu_p = \int_{-\infty}^{\infty} \varepsilon^p n_i(\varepsilon) d\varepsilon$; μ_0 and $\frac{\mu_1}{\mu_0}$ give the total number of states in the band and the center of gravity position B_d, respectively.
[61] B. Hammer and J. K. Nørskov, Surf. Sci. **343**, 211 (1995).
[62] B. Hammer, Y. Morikawa, and J. K. Nørskov, Phys. Rev. Lett. **76**, 2141 (1996).
[63] A. Kokalj, J. Mol. Graphics Modelling, 1999, Vol 17, pp. 176–179. Code available from http://www.xcrysden.org/.